NMR Imaging

E. RAYMOND ANDREW

Departments of Physics, Radiology, and Nuclear Engineering Sciences, University of Florida, Gainesville, Florida 32611

Received July 1, 1982

Readers of *Accounts* will be very familiar with the importance of nuclear magnetic resonance (NMR) as a branch of spectroscopy that furnishes structural and dynamical information of first importance in chemistry. Indeed no modern chemical laboratory is without its high-resolution NMR spectrometer. In most applications a small homogeneous specimen, typically less than 1 mL, of pure liquid or solid, is placed in a very uniform magnetic field, often uniform to a part in 10^9, and NMR spectra and relaxation times are recorded and interpreted. This may be termed *conventional* NMR.

In contrast with this conventional NMR spectroscopy, NMR imaging is concerned with applications to heterogeneous specimens, for example, parts of the human body, which are not small, and furthermore they are placed in a deliberately nonuniform magnetic field. The purpose of the nonuniform field is to label different parts of the specimen with different field strengths, so that they respond with recognizably different NMR frequencies, enabling the structure and internal processes of the specimen to be derived and displayed. We might notice at the outset that the high-resolution features of conventional NMR spectroscopy, with clusters of chemically shifted lines and spin multiplets, have not so far played a substantial role in NMR imaging.

Since hydrogen is the most abundant element in all living organisms, proton NMR lends itself particularly well as a method of investigation in biology and medicine. As a method of medical imaging we may note some of the special advantages that NMR imaging offers, namely that it does not use ionizing radiation, it is noninvasive, and indeed it is without known hazard; it is therefore a much safer means of imaging than modalities using X-rays, γ-rays, positrons, or heavy ions. We also note that in contrast with ultrasound the radiation penetrates bony structures without attenuation. Moreover, besides giving morphological information, NMR imaging gives additional diagnostic insights through relaxation parameters, which are not available from other imaging methods.

In the decade since the first primitive NMR images were obtained great strides have been made. The quality of pictures now approaches those from CT X-ray scanners, the number of hospital patients examined by NMR imaging nears the thousand mark, some 20 commercial companies in various countries are constructing prototype instruments for clinical evaluation, and the first whole-body NMR scanners are beginning to appear on the market at costs comparable with CT X-ray scanners.

Already in its short life a variety of names have been used in the literature to describe the subject, for example, NMR imaging, spin imaging, spin mapping, NMR zeugmatography, and NMR tomography. The reasons for the use of these names will be seen as we go along.

In writing this article it has been assumed that the reader is familiar with the fundamentals of conventional NMR, further details of which may be obtained from standard textbooks such as those referenced.[1-8] Notwithstanding the differences between conventional NMR and NMR imaging, the basic NMR phenomena remain the same in both applications and a formal description of the NMR equipment reads much the same for both. The object of interest is placed in the field of a magnet and is surrounded by a radio-frequency coil that is supplied from a radio-frequency generator. The NMR signal is picked up in a receiver coil, which may be the same coil as the transmitter coil, and after amplification and detection the signal is displayed. A dedicated minicomputer instructs the whole system, gathers the data, and performs all necessary calculations. The main differences in equipment are the much larger aperture magnets that are required for examining human subjects and the addition of coils to generate field gradients and facilities for manipulating the gradients.

Principles

If a 1-mL specimen of pure water is placed in the uniform magnetic field of a conventional NMR spectrometer, the proton NMR spectrum consists of a single sharp line of intrinsic width of about 0.1 Hz. If now a gradient of the order of 1 G/cm (10^{-2} T/m) is applied across the tube of water (Figure 1a) different parts of the specimen experience different field strengths. Remembering the direct proportionality between NMR frequency and field strength, we see that the NMR spectrum is a one-dimensional (1D) projection of proton density along the direction of the gradient.

This is further illustrated in Figure 1b for a specimen consisting of two tubes of water with the gradient applied along the line of centers. For a cluster of five

E. Raymond Andrew, a native of Boston, England, holds B.A., M.A., Ph.D., and Sc.D. degrees from Cambridge University. He did postdoctoral work at Harvard University as a Commonwealth Fund Fellow in 1948-1949, then took a Lectureship in Physics at the University of St. Andrews, and in 1954 became Professor of Physics at the University of Wales, Bangor, Wales. In 1964 he moved to Nottingham University as Lancashire-Spencer Professor of Physics. At Nottingham he was the Dean, Faculty of Science, from 1975 to 1978. He has recently taken up a new appointment as Graduate Research Professor at the University of Florida.

(1) Abragam, A. "Principles of Nuclear Magnetism"; Oxford University Press: Oxford, 1961.
(2) Abraham, R. J.; Loftus, P. "Proton and Carbon-13 NMR Spectroscopy"; Heyden: London, 1980.
(3) Andrew, E. R. "Nuclear Magnetic Resonance"; Cambridge University Press: Cambridge, 1969.
(4) Bovey, F. A. "NMR Spectroscopy"; Academic Press: New York, 1969.
(5) Carrington, A.; McLachlan, A. D. "Introduction to Magnetic Resonance"; Harper and Row: New York, 1967.
(6) Farrar, T. C.; Becker, E. D. "Pulse and Fourier Transform NMR"; Academic Press: New York, 1971.
(7) Günther, H. "NMR Spectroscopy"; Wiley: Chichester, UK, 1980.
(8) Pople, J. A.; Schneider, W. G.; Bernstein, H. J. "High Resolution Nuclear Magnetic Resonance"; McGraw-Hill: New York, 1959.

0001-4842/83/0116-0114$01.50/0

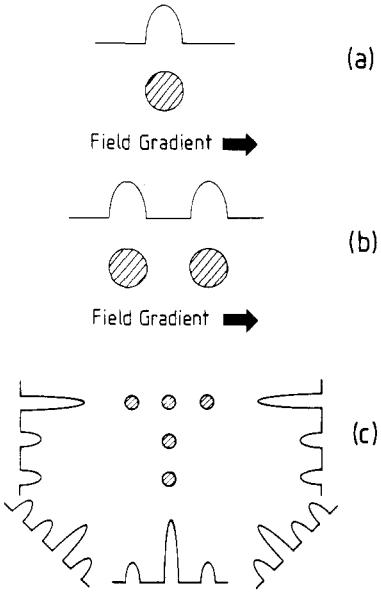

Figure 1. NMR spectrum of a structured specimen in a linear field gradient gives a one-dimensional projection of proton density along the gradient direction: (a) a single tube of water, (b) two tubes, and (c) five tubes arranged as a T.

tubes arranged in the form of a T (Figure 1c) 1D projections are shown for five different directions of application of the gradient. In fact for any irregular shaped object with an arbitrary internal distribution of mobile protons, the proton NMR spectrum in the presence of a field gradient gives a 1D projection or profile of proton density along the gradient direction.

NMR 1D projections were first investigated some years ago with simple glass and liquid structures by Gabillard,[9-11] who also studied their dynamic response. Field gradients are also an essential feature of the study of molecular diffusion in liquids by the NMR spin-echo method[12] and have also been used in the study of phase separation in ^{3}He–^{4}He solutions,[13] in methods of information storage,[14,15] and in the investigation of periodic structures by the NMR diffraction method.[16]

One-dimensional projections give some structural information, but for an image we require at least a two-dimensional (2D) representation of the NMR response. Better still we would like to have a 2D image of a thin defined slice in the object; a set of such images of coplanar slices in the object then provides a complete 3D representation of the object. The new feature in this use of field gradients is their manipulation to obtain an NMR image. In order to obtain 2D or 3D information by using this essentially 1D probe a time dependence is introduced by modulating, switching, or rotating the gradient.

First of all, the NMR response must be restricted to a plane or slice of the object, and there are two main ways of doing this. In the first[17] a linear field gradient is applied as indicated by the line PR in Figure 2a. The

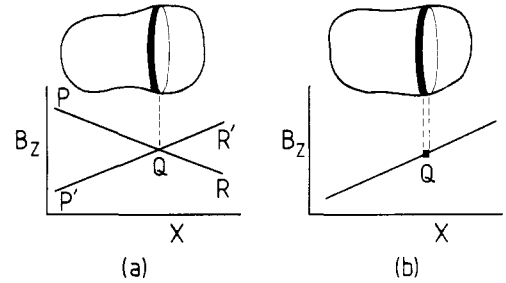

Figure 2. Slice selection (a) by alternating gradient and (b) by selective irradiation.

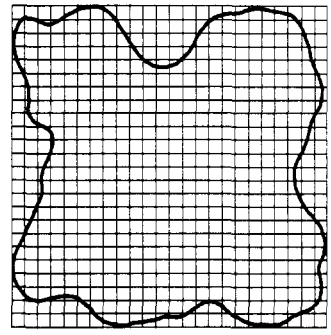

Figure 3. The image of a thin slice of any object may be divided into an $n \times n$ matrix of picture elements (pixels).

currents in the gradient coils are proportioned so that between P and Q a field is added to the main field of the magnet and between Q and R a field is subtracted. If the gradient currents are reversed, the field distribution is given by P′R′. If now the gradient coil currents are alternated at a low frequency, say 50 Hz, we have an alternating linear gradient and except at Q the magnetic field has an alternating small field superimposed on it. Consequently the NMR signal from the whole object is modulated at 50 Hz except in the "zero-field" plane in the vicinity of Q. If the NMR signal, after detection, is passed through a low-pass filter cutting off below 50 Hz, only the NMR response from a thin plane of nuclei at Q is retained, as indicated in Figure 2a.

The second approach uses the selective excitation method.[18] A linear field gradient is applied along the X direction (Figure 2b) and the object is irradiated on a well-defined narrow band of radio frequencies corresponding to the NMR frequencies of protons in just the narrow band of field values shown at Q. Consequently, only the protons in the plane at Q are excited. Alternatively we may arrange for all the nuclei in the object to be excited *except* those in the plane at Q, thus leaving a virgin plane of nuclei to be examined subsequently.

Let us suppose we have restricted the NMR response to a thin slice in the object by one of these methods; the slice is depicted in Figure 3. This slice and its 2D image may be divided, as indicated, into an $n \times n$ matrix of picture elements (pixels). Our task is now to evaluate the NMR response A_{pq} from each of these n^2 matrix elements. They may then be displayed as an image, for example on an oscillograph or a TV screen.

The most simple procedure consists in isolating and directly measuring the NMR response A_{pq} from one element pq at a time, moving sequentially from one to

(9) Gabillard, R. *C. R. Hebd. Seances Acad. Sci.* **1951**, *232*, 1551.
(10) Gabillard, R. *Phys. Rev.* **1952**, *85*, 694.
(11) See also ref 3, pp 134–136.
(12) Hahn, E. L. *Phys. Rev.* **1950**, *80*, 580.
(13) Walters, G. K.; Fairbank, W. M. *Phys Rev.* **1956**, *103*, 262.
(14) Anderson, A. G.; Garvin, R. L.; Hahn, E. L.; et al. *J. Appl. Phys.* **1955**, *26*, 1324.
(15) Andrew, E. R.; Finney, A.; Mansfield, P. Royal Radar Est. (RRE) Research Report PD/24/026/AT, 1970.
(16) Mansfield, P.; Grannell, P. K. *J. Phys. C.* **1973**, *6*, L422.
(17) Hinshaw, W. S. *Phys. Lett.* **1974**, *48A*, 78.
(18) Garroway, A. N.; Grannell, P. K.; Mansfield, P. *J. Phys. C.* **1974**, *7*, L457.

the next until all n^2 elements have been scanned. When the nomenclature of Brunner and Ernst[19] is used, such a procedure is called a *sequential point method.* Alternatively we might devise a procedure for isolating and recording a whole line or column of n elements simultaneously and then scan the plane line by line. Such a line-scanning procedure is called a *sequential line method.* Next we might devise a procedure for recording the NMR signal from all the n^2 elements in the plane simultaneously; this is called *planar imaging.* We would then be able to image the whole 3D object by looking at one slice after another; such a procedure is called a *sequential plane method.* Finally, we might devise a procedure that is able to record simultaneously the NMR signal from all n^3 cuboidal volume elements (voxels) into which it may be subdivided in 3D, and to do it in such a way that all n^3 voxels are evaluated. Such a method is called a *simultaneous method*[19] and represents full 3D imaging.

There are over a dozen different methods of NMR imaging, and in this Account we restrict attention to some of the more important features. A fuller account of all the methods is given elsewhere.[19,20]

Sequential Point Methods

One procedure for restricting the NMR signal to one small volume element is by extension of the alternating gradient method of slice selection to three dimensions. Apply three orthogonal alternating gradients along the X, Y, and Z directions. The small volume element at the intersection of the three orthogonal zero-field planes is the only element whose NMR signal is not modulated by the alternating gradients and it alone passes through the low-pass filter and is recorded and displayed. The volume element is traversed television-wise through a defined plane and the image may be synchronously displayed on the screen. This is the single sensitive point method of Hinshaw.[17] It is very simple and direct and requires no calculations or computer; it did in fact produce the first 3D NMR images.[21]

An alternative approach is to produce a spatial localization by auxiliary coils in the magnet so that only a small region responds at the NMR frequency. This is the FONAR (focused nuclear resonance) method of Damadian,[22,23] which generated the first human whole-body NMR images and became the basis of the first commercial NMR whole-body scanner.

Sequential point methods are inevitably slow. Well-resolved images require n to be at least 128. Thus if each pixel takes, say, 0.3 s to record, the image of one slice takes an hour or so to obtain.

Sequential Line Methods

A considerable improvement in imaging time is achieved by imaging a line of elements simultaneously. One way of doing this is to apply two orthogonal alternating gradients along the Y and Z directions. The intersection of the two orthogonal slices so defined gives a line of elements along the X direction. With a static gradient applied along the X direction the Fourier-transformed free induction decay (FID) following an NMR pulse gives the 1D projection of nuclear density along the X direction, recording all n elements in the line simultaneously and giving the customary n-fold Fourier-transform time advantage. Well-resolved images of objects up to 10-cm diameter were obtained with this method in several minutes.[24] A proton NMR image of a lemon[25,26] is shown in Figure 4 and that of a live human wrist[27,28] in Figure 5.

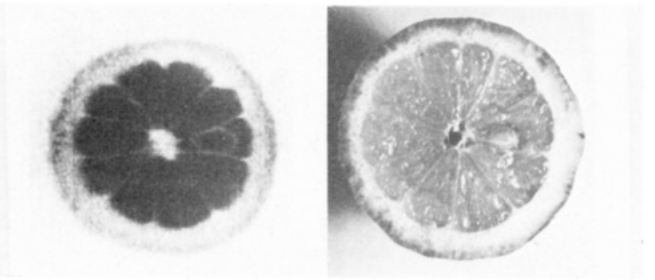

Figure 4. Thin transverse section proton NMR image of an intact lemon (left) and photograph of actual section cut subsequently (right).[25,26] Reproduced with permission from ref 26. Copyright 1980, The Royal Society, London.

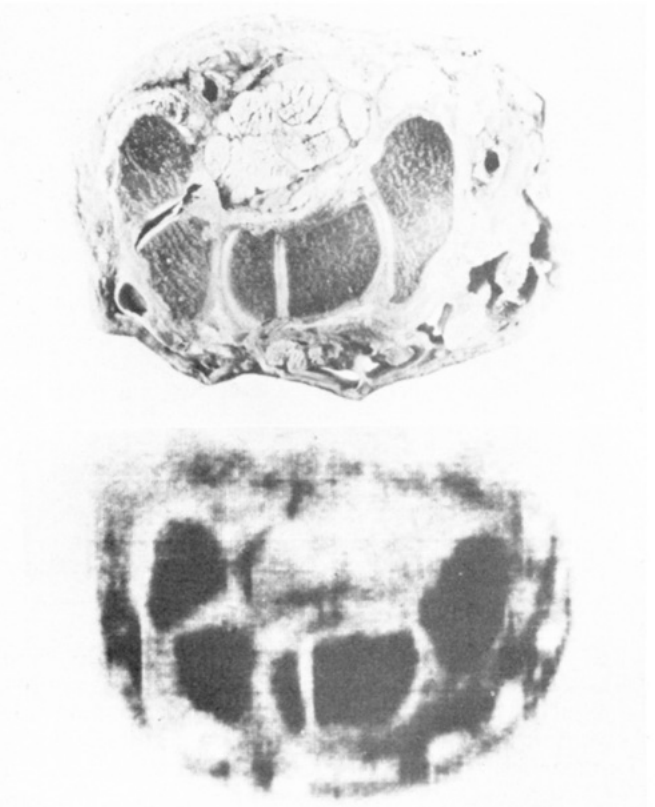

Figure 5. Thin transverse proton NMR image through the left wrist of Dr. P. A. Bottomley (above) anda photograph of a matching section from a cadaver wrist (below).[27,28] Reproduced with permission from ref 26. Copyright 1980, The Royal Society, London.

(19) Brunner, P.; Ernst, R. R. *J. Magn. Reson.* **1979**, *33*, 83.
(20) Andrew, E. R. 1982 IEEE Proceedings International Workshop on Physics and Engineering in Medical Imaging.
(21) Hinshaw, W. S. *J. Appl. Phys.* **1976**, *47*, 3709.
(22) Damadian, R.; Goldsmith, M.; Minkoff, L. *Physiol. Chem. Phys.* **1977**, *9*, 97.
(23) Damadian, R. *Philos. Trans. R. Soc. London, Ser. B* **1980**, *289*, 489.
(24) Andrew, E. R.; Bottomley, P. A.; Hinshaw, W. S.; Holland, G. N.; Moore, W. S.; Simaroj, C. *Phys. Med. Biol.* **1977**, *22*, 971, 1291.
(25) Andrew, E. R.; Bottomley, P. A.; Hinshaw, W. S.; et al. *Magn. Reson. Relat. Phenom., Proc. Congr. Ampere, 20th, 1979*, 53.
(26) Andrew, E. R. *Philos. Trans. R. Soc. London, Ser. B* **1980**, *289*, 471.
(27) Hinshaw, W. S.; Bottomley, P. A.; Holland, G. N. *Nature (London)* **1977**, *270*, 722.
(28) Hinshaw, W. S.; Andrew, E. R., Bottomley, P. A.; Holland, G. N.; Moore, W. S.; Worthington, B. S. *Neuroradiology* **1978**, *16*, 607.

An alternative procedure is to apply selective excitation in two dimensions. A field gradient is applied along the Z direction and a thin slice of nuclei is selectively isolated. When the gradient is switched rapidly to the Y direction a thin line of spins along X is selectively excited in the chosen slice. Finally, the gradient is switched along X and the FID of this line of excited nuclei is read, giving the nuclear distribution along this line. This method also enjoys the Fourier-transform advantage over sequential point methods. It was used to obtain the first human abdominal NMR image.[29]

An image of $n \times n$ pixels requires an FID to be recorded for each of the n lines of the picture. If each line takes a second or so to record, then with $n = 128$, the minimum time taken to obtain the data for the image is about 2 min. Each line can be Fourier-transformed while successive lines are being scanned and the image on the display is built up line by line.

Planar Imaging

The most successful human whole-body NMR images to date have been obtained by methods in this category. In these methods NMR signals are gathered from all the nuclei in a defined slice of the object all the time and therefore have an inherent advantage in sensitivity over the methods so far described that gather NMR signals only from a point or a line at a time.

The first published NMR image, by Lauterbur,[30] of the proton density distribution in two tubes of water, provides the basis for the first method in this category, called the 2D projection–reconstruction method. A slice in the object is first defined by one of the two ways described earlier. A linear field gradient is then applied in the plane of this defined slice. The FID is read and Fourier-transformed to give a 1D projection of proton density of this slice in the direction of the gradient. The field gradient is now applied in successively different directions around an axis, giving a series of 1D projections of the slice as illustrated in Figure 1c. The situation is thus closely similar to that in CT X-ray scanning and by back projection or other methods an image can be reconstructed by computer of the nuclear density in the selected slice, perpendicular to the axis about which the gradient is rotated.

In order to obtain data for an image with $n \times n$ pixels, at least n^2 NMR readings must be taken. This may, for example, be achieved by applying the gradient in n successive directions with equally spaced angles and recording the FID for each with n data points.

The second method in this category is 2D Fourier imaging;[31] readers will note a close similarity between its procedures and those of 2D Fourier-transform NMR spectroscopy. In this method a slice in the object in the XZ plane is first defined. A field gradient is then applied along the X direction in this defined plane for a time t_X, after which it is switched along the Z direction. The FID is then read as a function of time t_Z. In this method the gradient is not rotated; it is simply directed along either X or Z only, but the time t_X for which the gradient is applied along X is progressively increased, and for each value of t_X the FID is read as a function of t_Z. If for n different values of t_X the FID is read with n data points t_Z, a total of n^2 readings is obtained. By double Fourier transformation with respect to the variables t_X and t_Z, the $n \times n$ pixels of the image are evaluated.

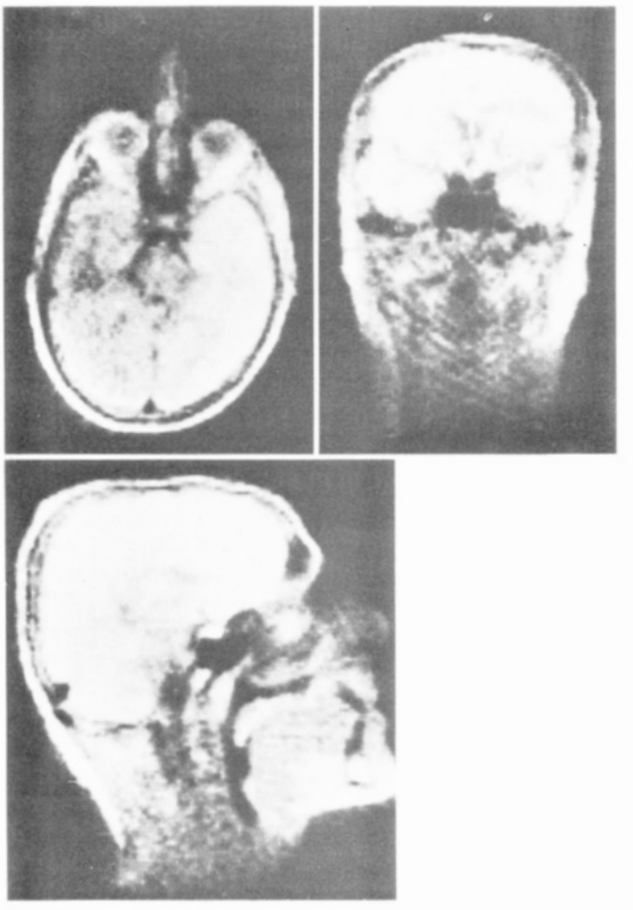

Figure 6. Transverse, coronal, and sagittal proton NMR tomographic images of the head of a normal human subject.[33] Reproduced with permission from ref 33. Copyright 1980, Raven Press.

It will be noted that during the preparation time t_X the nuclear spins precess at different frequencies according to the particular magnetic field they experience, and this leaves their phases at the end of t_X dependent on their spatial coordinate x. In a variant of this method the time t_X is held constant but the value of the field gradient is progressively incremented n times, which has the same effect; this has been named the spin-warp method.[32] It has the practical merit of keeping the timing sequences fixed.

In both methods just described, namely 2D projection–reconstruction and 2D Fourier imaging, n FID's must be recorded. The minimum time required to obtain the data for the image (minimum performance time) is therefore approximately the same as in sequential line methods, namely several minutes. On the other hand, each FID is generated by all $n \times n$ volume elements in the defined plane, whereas in the sequential line methods each FID is obtained from just the n elements of the line under examination. The two planar imaging methods should therefore enjoy substantial superiority in sensitivity compared with sequential line methods, and this appears to be borne out in practice.

(29) Mansfield, P.; Pykett, I. L.; Morris, P. G.; Coupland, R. E. *Br. J. Radiol.* **1978**, *51*, 921.
(30) Lauterbur, P. C. *Nature (London)* **1973**, *242*, 190.
(31) Kumar, A.; Welti, D.; Ernst, R. R., *J. Magn. Reson.* **1975**, *18*, 69.
(32) Edelstein, W. A.; Hutchison, J. M. S.; Johnson, G.; Redpath, T. W. *Phys. Med. Biol.* **1980**, *25*, 751.

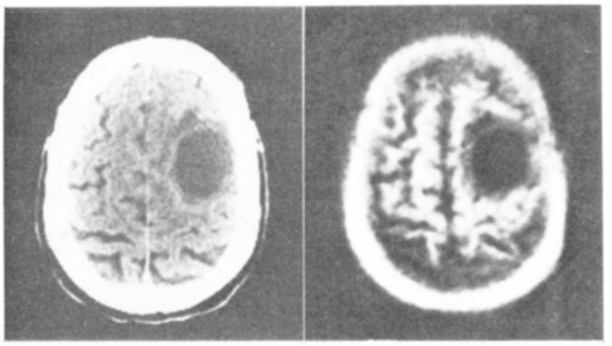

Figure 7. CT X-ray scan (left) and proton NMR scan (right) of a 70-year-old man with a glioblastoma multiforme.[37] The NMR scan shows strong relaxation discrimination between grey and white matter of the brain. The loss of white matter in the tumor is demonstrated. Reproduced from ref 37 with permission of the authors, Royal Post Graduate Medical School Hammersmith, Picker International, and the Editor of *The Lancet*, London. Copyright 1981, Little Brown.

The best human whole-body NMR images to date have been obtained by these two methods. When the projection–reconstruction method in a plane defined by an alternating gradient is used well-resolved images of transverse, coronal, and sagittal sections of the head have been obtained in Nottingham in 2 min[33,34] (Figure 6) and later of the chest and heart[35] and abdomen[36] also. When the projection–reconstruction method in a plane defined by selective excitation is used, well-resolved images of the head have been obtained at Hammersmith Hospital, London,[37-39] showing a remarkable discrimination between grey and white matter of the brain through exploitation of their relaxation-time differences (Figure 7). The method also has been extended to imaging of the chest and abdomen.[39] Using the 2D Fourier-imaging (spin-warp) method, a large number of whole-body images, particularly of the abdomen, have been obtained in Aberdeen.[40] In these three centers in Britain, where most of the early clinical trials have been carried out, nearly 1000 patients have now been examined and the diagnostic value of NMR imaging has been clearly demonstrated.

A third planar imaging method utilizes a gradient of the radio-frequency magnetic field in conjunction with a gradient of the laboratory magnetic field. This method is called rotating frame imaging[41] and has yielded preliminary 2D projection images of phantoms; at the time of writing the method has not yet been fully developed.

We have seen that the planar imaging methods described so far require n successive FID's to be recorded, and with $n = 128$, this dictates a minimum performance time of a few minutes to obtain an image. By comparison good CT X-ray images can be obtained in a few seconds. In pursuit of faster NMR imaging times Mansfield[42] has proposed the echo planar imaging method. A slice in the object in the XZ plane is first defined by selective excitation. A field gradient is then applied in this defined slice, in, say, the Z direction. This gradient is periodically reversed, bringing the precessing nuclei periodically back into phase as spin echoes that are Fourier transformed to provide a periodicity along Z. In fact the nuclear density behaves as if it were heaped up in strips across the slice, perpendicular to Z. If then a small gradient is added along the X direction these strips are read obliquely in a unique manner giving the proton-density distribution of the whole plane in a single FID. In this method all nuclei in the plane contribute to the image so that the inherent sensitivity is as good as the other planar-imaging methods described earlier, but the minimum performance time is much shorter. Indeed the minimum performance time may be as little as the duration of a single FID, typically 30 ms.

The method has been shown to work and has produced images of 32×32 pixels of objects up to 10 cm in size.[43] This opens up the possibility of producing NMR images of moving objects in real time, and the first real-time NMR images were recently demonstrated of a moving phantom, a live rabbit with a beating heart, and a human arm rotating.[44] If this method is successfully scaled up to human whole-body sizes, it has an important future in providing real-time clinical NMR images.

3D Imaging

The imaging of a single slice, or of a small number of slices, in a structured object such as the human head or body may give sufficient information for medical purposes. If, however, a complete NMR measurement of all n^3 voxels characterizing the 3D object is desired, a sequential plane method may take a long time with $n \sim 100$. In this situation simultaneous or true 3D imaging methods have their attractions.

In a true 3D imaging method NMR signals are gathered from the whole 3D object in every measurement; they are collected and processed in such a way that the NMR signal from all n^3 volume elements is determined. The NMR image of any selected slice of arbitrary orientation may then be displayed. The 3D image of the whole object may be displayed as a series of n 2D images of coplanar slices, each with $n \times n$ pixels.

One procedure is to extend the projection–reconstruction method to 3D. A linear field gradient is applied successively in n^2 directions disposed isotropically around the object. For example, n projections may be taken round each of n longitudes, or the direction of the gradient may pursue a spiral path from pole to equator.[45] The NMR response is measured with n data points for each of the n^2 projections, giving a total of n^3 data values. The 3D reconstruction of the n^3 voxels characterizing the object from these n^3 data values calls for powerful computing facilities if it is to be accom-

(33) Holland, G. N.; Hawkes, R. C.; Moore, W. S. *J. Comput. Assist. Tomogr.* **1980**, *4*, 429.
(34) Hawkes, R. C.; Holland, G. N.; Moore, W. S.; Worthington, B. S. *J. Comput. Assist. Tomogr.* **1980**, *4*, 577.
(35) Hawkes, R. C.; Holland, G. N.; Moore, W. S.; Roebuck, E. J.; Worthington, B. S. *J. Comput. Assist. Tomogr.* **1981**, *5*, 605.
(36) Hawkes, R. C.; Holland, G. N.; Moore, W. S.; et al. *J. Comput. Assist. Tomogr.* **1981**, *5*, 613.
(37) Doyle, F. A.; et al. *Lancet* **1981**, Jul 11, 53.
(38) Young, I. R.; et al. *Lancet* **1981**, Nov 14, 1063.
(39) Young, I. R.; et al. *J. Comput. Assist. Tomogr.* **1982**, *6*, 1.
(40) Smith F. W.; Mallard, J. R.; Reid, A.; Hutchison, J. M. S. *Lancet* **1981**, May 2, 963.
(41) Hoult, D. I. *J. Magn. Reson.* **1979**, *33*, 183.
(42) Mansfield, P. *J. Phys. C.* **1977**, *10*, L55.
(43) Ordidge, R. J.; Mansfield, P.; Coupland, R. E. *Br. J. Radiol.* **1981**, *54*, 850.
(44) Ordidge, R. J.; Mansfield, P.; Doyle, M.; Coupland, R. E. *Proc. Int. Symp. NMR Imaging* **1981**, 89.
(45) Lai, C. M.; Lauterbur, P. C. *J. Phys. E.* **1980**, *13*, 747.

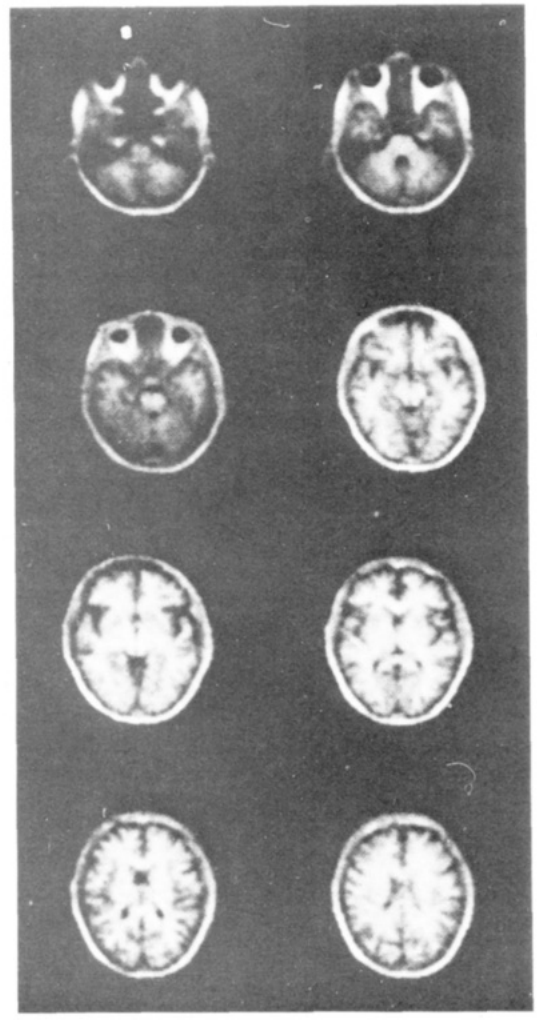

Figure 8. True three-dimensional NMR imaging of a normal human head, showing images of selected transverse planes. Reproduced from ref 47 with permission of Dr. W. S. Hinshaw and the editor.

plished in a reasonable time. The feasibility of the method was first demonstrated by Lai and Lauterbur[45,46] for $n = 33$. Fourier imaging has also been extended in 3D to the true NMR imaging of a live human head[47] with $n = 64$, generating a striking series of coplanar images of slices about 3 mm thick in a total imaging time of 40 min (Figure 8).

Nature of the Image: Relaxation Effects

It is natural to ask what is actually being displayed in the NMR image. The image is not just a 2D representation of proton density $\rho(x,y,z)$ at each point x,y,z in the defined slice of the object. Rather it is a spatial representation of the NMR signal. The NMR signal is certainly proportional to the proton density at each point, since the nuclear magnetization at each point is proportional to the proton density. However in general the NMR signal from the volume element at x,y,z will be given by

$$[\rho\ f(T_1,T_2,v,\ ...)]_{xyz}$$

and the precise form of the function f of the relaxation times T_1 and T_2, fluid-flow velocity v, and other parameters will depend on the method of measurement.

It is instructive to recall that in conventional NMR spectroscopy there are many ways of recording an NMR spectrum with consequent differences in the information displayed. We may apply a 90° pulse, record the FID, Fourier transform, wait $5T_1$, and repeat until a spectrum of adequate signal/noise is accumulated. In this case the intensity of the spectral components may well be proportional to the numbers of nuclei concerned. Alternatively if we pulse more frequently a driven equilibrium is obtained and spectra are generated more rapidly, but the intensity of each component depends now on T_1 and T_2 of the nuclei concerned. If we apply a 180° inverting pulse and wait an interval τ before applying the 90° read pulse, the sign and intensity of the Fourier-transformed spectral components depend on their individual T_1. If in a nonuniform field we apply a spin-echo sequence, the echo envelope depends on T_2 and on any diffusion or flow of the nuclei.

In NMR imaging also simple well-separated 90° pulses may be used to generate images that reflect primarily the nuclear density of fluid and soft components; driven-equilibrium methods may be used to secure faster data collection, but with a greater dependence on T_1 and T_2; inversion–recovery procedures with judiciously chosen τ gave a T_1-modulated display that discriminates differences in T_1 between different normal tissues or between normal and diseased tissue; inversion–recovery also enables T_1 to be computed for each pixel, so that an image of T_1 values rather than NMR signal itself can be displayed; a spin–echo sequence allows a T_2-modulated image to be obtained. A series of images,[39] which contrasts the effects of these different procedures for a normal head, is shown in Figure 9.

The practical diagnostic significance of T_1 in clinical applications is underlined by the observation by Damadian,[48] subsequently verified by other workers, that cancerous tissue has substantially longer proton relaxation times than in corresponding normal tissue.

Resolution and Imaging Time

It is important to note that there is a close relationship between the resolution in the image and the time taken to acquire the image. It it is desired to improve the resolution by, say, a factor of 2 in all three dimensions, each voxel is reduced in volume by a factor of 8. If other parameters are kept constant, the time required to obtain an NMR signal of the same signal/noise ratio as before is therefore increased by a factor of 64. In fact, the imaging time increases as n^6. If it is merely desired to improve the resolution in the image plane while the same slice thickness is retained, the picture time increases only as n^4. In either case one pays dearly in acquisition time for much improved resolution.

It is clear, therefore, that the efficient gathering of NMR information is of prime importance if imaging times are to be as short as possible without sacrifice of signal/noise ratio or resolution. Moreover one should operate at as high a field and frequency as possible in order to enjoy the higher signal/noise ratio that this endows.[1,3]

In traditional microscopy the limit of resolution is set by the wavelength of the illuminating radiation. If our NMR operating frequency is 10 MHz, the free-space wavelength of the electromagnetic radiation is 30 m,

(46) Lai, C. M.; Lauterbur, P. C. *Phys. Med. Biol.* **1981**, *26*, 851.
(47) Buonanno, F. S.; Pykett, I. L.; Hinshaw, W. S.; et al. *Proc. Int. Symp. NMR Imaging* **1981**, 147.
(48) Damadian, R. *Science (Washington, D.C.)* **1971**, *171*, 1151.

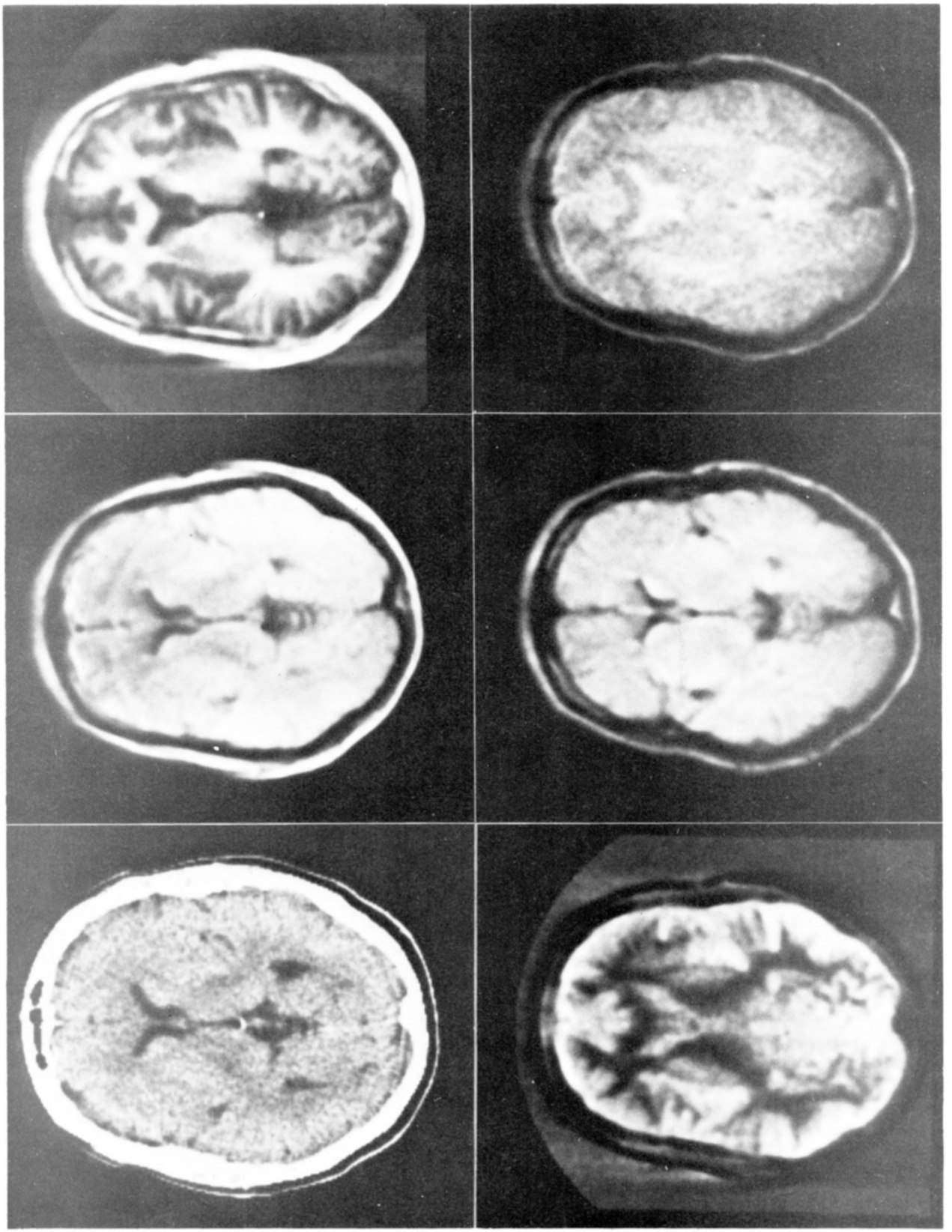

Figure 9. Normal human brain transverse scans.[39] Same subject, different scan conditions. Top row from left: (a) CT X-ray, (b) NMR proton density, (c) T_1 modulated. Bottom row from left: (d) T_1, (e) T_2 (short pulse interval τ), (f) T_2 (long τ). Reproduced in part from ref 39 with permission of the authors, Royal Post Graduate Medical School Hammersmith, Picker International, and Raven Press. Copyright 1982, Raven Press.

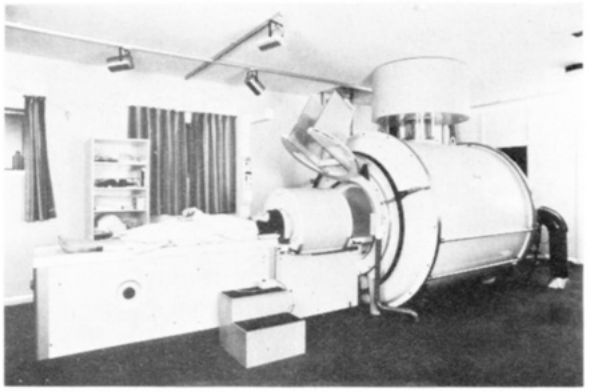

Figure 10. The NMR head and body scanner, using a superconducting magnet, at the Royal Post Medical School Hammersmith. Reproduced with the permission of the RPGMS and Picker International.

and this clearly has nothing to do with the resolution in the NMR images. In fact the spatial discrimination and resolution are determined by the magnetic field and its gradient, while the electromagnetic field serves to detect the NMR phenomenon. Both fields must be conjoined in the object, a fact that led Lauterbur[30] to coin the word "zeugmatography" to describe NMR imaging from the Greek word zeugma, "that which joins together".

Magnets

For objects up to 10 cm in size it is possible to use modified versions of magnets employed in conventional NMR spectroscopy. On the other hand, for human whole-body NMR imaging magnets with a much larger aperture are needed. Analysis of the penetration of electromagnetic radiation into living tissue[49] suggests that above about 15 MHz problems of attenuation and phase distortion become significant. For proton NMR this implies the use of a magnetic field not more than about 0.35 T for whole body imaging.

A common type of resistive magnet for whole-body imaging consists of four air-core coils approximating to a "spherical" configuration.[26] Standing 2 m high they have an access of 60 cm through end coils to accept a horizontal patient. Such magnets generate 0.1 T with about 20 kW of electrical power and can sometimes be operated up to 0.15 T. Above this field strength the power consumption of resistive magnets becomes prohibitive.

For higher field strengths superconducting magnets are more attractive and are now available commercially for whole-body imaging. The example shown in Figure 10 has a straight through horizontal bore of 1-m diameter.[50]

Questions of Safety

There appear to be three conceivable sources of hazard in human NMR tomography that demand attention, namely the effects of static magnetic fields, time-varying magnetic fields, and radio-frequency fields.

There is a substantial literature on biological effects of magnetic fields. Scientific workers in particle accelerator laboratories have been exposed to magnetic fields of the order of 2 T without ill effects. So far no volunteer or patient who has been imaged by NMR has reported significant effects.[63] In Britain the National Radiological Protection Board issued interim guidance[51] on safe procedures in NMR clinical imaging in 1980 and recommended that the static magnetic field B should not exceed 2.5 T. In the United States the matter has been discussed by Budinger,[52] and the Bureau of Radiological Health has recently[53] recommended a limit of 2 T. Practical systems are in fact well below these limits.

As we have seen, some imaging methods use alternating or rapidly switched magnetic field gradients. Although no ill effects have been reported there is less evidence here and more reason to be careful since a change of magnetic flux might induce currents in the nervous system, the brain, and the heart. Here the NRPB[51] recommends a maximum value of dB/dT of 20 T s^{-1}, while the BRH[53] recommends 3 T s^{-1}.

The main consequence of the radio-frequency electromagnetic field is its heating effect. Many years of experience with short-wave diathermic therapy for rheumatism and other disorders have revealed no hazard in its proper application. The recommended[51-53] maximum mean radio-frequency power for NMR clinical imaging is 2 W/kg.

The whole question of safe limits of working will be continually monitored in the light of experience. It does, however, seem likely that within the limits recommended human whole-body NMR imaging will be free from hazard.

The Future

The most immediate and exciting perspective is the outcome of the clinical trials currently in progress in many hospitals in the world. Early results are encouraging, and in a few years it will become clear just how useful this modality of medical imaging is to the medical profession in the diagnosis and treatment of disease. The verdict of clinicians will be crucial to the future commercial development of NMR scanners and their place in hospital practice.

Protons have been the favorite nuclei for NMR imaging so far on account of their very favorable NMR characteristics coupled with the high concentration of hydrogen in living systems. Nevertheless, other nuclei have potential interest. Some imaging work has been done with ^{19}F, ^{23}Na, and ^{31}P; other nuclei that may be of interest in the future include ^{2}H, ^{13}C, ^{14}N, and ^{15}N. Since these nuclei have much weaker NMR sensitivity in living systems, a significantly lower image resolution will be inevitable compared with proton imaging.

The great majority of NMR imaging to date has ignored the high-resolution structure of the NMR response, which in conventional NMR spectroscopy is its source of strength. If it were possible to obtain images of particular chemically shifted lines in the NMR spectra one would then have images which display the distribution of particular chemical species in the defined slice of the structured object. Some preliminary experiments were carried out with high-resolution proton

(49) Bottomley, P. A.; Andrew, E. R. *Phys. Med. Biol.* **1978**, *23*, 630.
(50) Young, I. R.; et al. *Proc. Int. Symp. NMR Imaging* **1981**, 949
(51) "Exposure to Nuclear Magnetic Resonance Clinical Imaging"; UK National Radiological Protection Board: Harwell, Didcot, UK, 1980.
(52) Budinger, T. F. *IEEE Trans. Nucl. Sci.* **1979**, *NS-26*, 2821.
(53) "Guidelines for Evaluating Electromagnetic Risk for Trials of Clinical NMR Systems". U.S. Bureau of Radiological Health: Washington DC, Feb 12, 1982.

lines in a simple phantom by Lauterbur,[54] who subsequently obtained images, by the projection–reconstruction method, of ^{31}P nuclei in particular metabolites.[55] The ^{31}P chemical shifts are an order of magnitude larger than proton chemical shifts so that the field gradients may more easily be applied without obliterating the spectral structure. It is clearly important in such applications to work in the highest possible magnetic field in order to open up the chemically shifted spectra.

We should note in passing the complementary nature of such work to "topical" NMR spectroscopy[56] in which high-resolution NMR spectra of ^{31}P and other nuclei are obtained from well-defined small volumes in the human body using auxiliary magnet coils.

Other potential applications of NMR imaging include the investigation of fluid flow,[57] the development of NMR microscopy for NMR imaging of small objects both animate and inanimate,[58] the nondestructive examination of the interior of food products, the diffusion of water in soil and in building materials,[59] and the imaging and interior examination of solid materials in conjuction with high-resolution solid-state NMR line-narrowing procedures.[60]

Finally we may note that the ideas of NMR imaging may be extended to the imaging of unpaired electrons using electron spin resonance (ESR). Such extension has been applied to the study of the distribution of defects in diamonds[61] and of free radicals in solids.[62]

(54) Lauterbur, P. C.; Kramer, D. M.; House, W. V.; Chen, C. N. *J. Am. Chem. Soc.* **1975**, *97*, 6866.
(55) Bendel, P.; Lai, C-M.; Lauterbur, P. C. *J. Magn. Reson.* **1980**, *38*, 343.
(56) Gordon, R. E. *Phys. Bull.* **1981**, *32*, 178.
(57) Garroway, A. N. *J. Phys. D* **1974**, *7*, L159.
(58) Mansfield, P.; Grannell, P. K. *Phys. Rev. B: Solid State* **1975**, *12*, 3618.
(59) Gummerson, R. J.; Hall, C.; et al. *Nature (London)* **1979**, *281*, 56.
(60) Richards, R. E.; Packer, K. J. "Nuclear Magnetic Resonance Spectroscopy in Solids"; The Royal Society: London, 1981.
(61) Hoch, M. J. R.; Day, A. R. *Solid State Commun* **1979**, *30*, 211.
(62) Hoch, M. J. R. *J. Phys. C* **1981**, *14*, 5659.
(63) Smith, F. W. *Lancet* **1982**, Apr 24, 974.

Thermodynamics of Metastable Intermediates in Solution

J. PETER GUTHRIE[1]

Department of Chemistry, University of Western Ontario, London, Canada, N6A 5B7

Received March 5, 1982 (Revised Manuscript Received October 4, 1982)

Chemical reactions frequently involve short-lived intermediates that are never present at detectable concentrations, yet are obligatory stages on the path from starting materials to products. There is as yet no general procedure for determining the free energy level of such an intermediate relative to the starting materials. This situation should be contrasted with that for starting materials and products or for intermediates which accumulate to detectable levels, where there are numerous methods for determining the relative free energy levels. If all else fails it will always be possible, for isolable starting materials and products, to determine the appropriate thermodynamic quantities (heat of formation, standard entropy, and so the free energy of formation) to permit calculation of the free energy change for the reaction.

The lack of a suitable method for intermediates that are too unstable to accumulate to detectable levels has been a serious nuisance, since such intermediates occur in most of the important reactions in organic chemistry. Such species are found in acyl-transfer reactions (tetrahedral intermediates), reactions α to carbonyl groups (enols), and phosphoryl-transfer reactions (pentacoordinate intermediates). For all such reactions involving simple substrates, the intermediates are detectable only under very special circumstances.

We have been engaged for several years[2-14] in developing methods that will provide at least a partial solution to this problem and believe that we now have developed a satisfactory general approach that permits the evaluation of the free energy level of any intermediate whose instability derives from the presence of a hydroxyl group but whose analogue with an alkoxyl group is stable. Thus far we have concentrated on reactions in aqueous solution, but in principle there is no reason why the method cannot be extended to other solvents. This includes a large fraction of the meta-

J. Peter Guthrie was born in Port Elgin, Ontario, Canada, in 1942. He received his undergraduate education at the University of Western Ontario and his Ph.D. from Harvard University in 1968. After a year as a NRC of Canada postdoctoral fellow at Princeton University he joined the faculty at the University of Western Ontario, where he is now Professor of Chemistry.

(1) E. W. R. Steacie Fellow, 1980–1982.
(2) Guthrie, J. P. *J. Am. Chem. Soc.* **1973**, *95*, 6999.
(3) Guthrie, J. P. *J. Am. Chem. Soc.* **1974**, *96*, 3608.
(4) Guthrie, J. P. *Can. J. Chem.* **1975**, *53*, 898.
(5) Guthrie, J. P. *Can. J. Chem.* **1976**, *54*, 202.
(6) Guthrie, J. P. *J. Am. Chem. Soc.* **1977**, *99*, 3991.
(7) Guthrie, J. P. *J. Am. Chem. Soc.* **1978**, *100*, 5892.
(8) Guthrie, J. P. *Can. J. Chem.* **1977**, *55*, 3562.
(9) Guthrie, J. P. *Can. J. Chem.* **1978**, *56*, 962.
(10) Guthrie, J. P. *Can. J. Chem.* **1978**, *56*, 2342.
(11) Guthrie, J. P. *Can. J. Chem.* **1979**, *57*, 236.
(12) Guthrie, J. P.; Cullimore, P. A. *Can. J. Chem.* **1979**, *57*, 240.
(13) Guthrie, J. P. *Can. J. Chem.* **1979**, *57*, 454.
(14) Guthrie, J. P.; Cullimore, P. A. *Can. J. Chem.* **1980**, *58*, 1281.

0001-4842/83/0116-0122$01.50/0